



Published in final edited form as:

Tissue Eng Part A. 2009 September ; 15(9): 2315–2324. doi:10.1089/ten.tea.2008.0391.

Zonal chondrocytes seeded in a layered agarose hydrogel create engineered cartilage with depth-dependent cellular and mechanical inhomogeneity

Kenneth W. Ng^{*}, Gerard A. Ateshian^{**}, and Clark T. Hung^{*,†}

^{*}Cellular Engineering Laboratory, Department of Biomedical Engineering Columbia University, New York, NY 10027, USA

^{**}Musculoskeletal Biomechanics Laboratory, Department of Mechanical Engineering Columbia University, New York, NY 10027, USA

Abstract

It was hypothesized that zonal populations of chondrocytes seeded into a bilayered scaffold with initially prescribed depth-varying, compressive material properties will lead to a biomimetic cartilage tissue construct with depth-dependent cellular and compressive mechanical inhomogeneity similar to the native tissue. Superficial zone chondrocytes (SZCs) and middle/deep zone chondrocytes (MDZCs) were isolated and encapsulated with 2% or 3% agarose to form single layered constructs of 2% SZC, 3% SZC, 2% MDZC; bilayered constructs of 2% SZC / 2% MDZC and 3% SZC / 2% MDZC; and 2% mixed chondrocyte controls. For SZCs on day 42, increased GAG and collagen was found with increased agarose concentration, and when layering with MDZCs. Superficial zone protein increased with increasing agarose concentration in bilayered constructs. For MDZCs, increased GAG content and regulation of cell proliferation was observed when layering with SZCs. Bilayered constructs possessed a depth-dependent compressive modulus that was qualitatively similar to native articular cartilage whereas controls showed a U-shaped profile with stiffer peripheral edges and softer middle region. This study is the first to create an engineered cartilage tissue with both depth-varying cellular and mechanical inhomogeneity. Future studies will determine if replicating inhomogeneity is advantageous in clinical uses of tissue engineered cartilage.

Introduction

Biomimetic approaches have often been adopted for tissue engineering, using the native tissue as inspiration for the design of engineered replacements (as reviewed in (1–3)). For articular cartilage, the focus has largely been on engineering constructs that exhibit the average, whole-tissue material and biochemical characteristics of native cartilage (e.g., (4–8)), a feat that has posed a greater challenge than originally appreciated. While the stratification of articular cartilage, namely the depth-varying material and biochemical properties (9,10) as well as the zonal cell populations (11), has been well-characterized, its role in cartilage development and load-bearing function is not entirely understood. In this regard, it is uncertain whether such tissue stratification of engineered cartilage is clinically needed for the successful repair of cartilage. The ability to create a functional cartilage surrogate which mimics both the whole-tissue properties as well as the inhomogeneous, depth-varying distribution of native cartilage may therefore be valuable from a basic science as well as tissue engineering perspective,

[†]Corresponding Author: Dr. Clark T. Hung, Columbia University, Department of Biomedical Engineering, 1210 Amsterdam Avenue, 351 Engineering Terrace, MC 8904, New York, NY 10027, Tel: (212) 854-6542, Fax: (212) 854-8725, E-mail: cth6@columbia.edu.

providing a model system to better understand the functional role of depth-dependent properties.

Constructs replicating the native distribution of chondrocyte populations have shown success in preserving the phenotype of superficial, middle, and deep zone cells in engineered cartilage (12–14). However, the reported depth-dependent material properties were not the same as the native tissue (15) and the overall material properties were generally poor (13,14,16). Our previous work using bilayered hydrogel constructs of different agarose concentrations, leading to differing initial material properties in each layer, and seeded with a mixed chondrocyte population, showed some promise as tissue constructs grew to exhibit increasing stiffness with tissue depth (17). In this study, we build on our early work by incorporating specific zonal chondrocyte populations in each layer. This approach utilizes new culture techniques that have successfully generated cartilage constructs with physiologic material and GAG levels (18). It is hypothesized that zonal populations of chondrocytes seeded into a bilayered scaffold with initially prescribed depth-varying, compressive material properties will lead to a biomimetic cartilage tissue with depth-dependent cellular and compressive mechanical inhomogeneity similar to the native tissue. This research aims to create a model system that can subsequently be used in future *in vivo* studies to evaluate the necessity for depth-varying zonal chondrocyte populations and spatial material properties in creating an engineered cartilage that can restore the lubrication and weight-bearing abilities of osteoarthritic diarthrodial joints.

Materials and Methods

Engineering of Tissue Constructs

Zonal populations of articular chondrocytes were isolated from bovine calf knee cartilage based on (12). Full-thickness cartilage blocks were excised from the femoral condyles and patello-femoral groove with the articular surface considered the “top” of the tissue blocks and the bone/calcified cartilage considered as the “bottom.” Bone and the bottom 15% of the blocks were excised and discarded. The top 10% of the cartilage, including the articular surface, was removed for isolation of superficial zone chondrocytes. The bottom 50% of the remaining tissue block was harvested for isolation of middle and deep zone chondrocytes. For isolating mixed populations of chondrocytes, knee tissue with only the bone and calcified region removed were used. For comparison with previous studies (e.g., (18)), bovine calf carpometacarpal (CMC) cartilage was also harvested.

Chondrocytes were isolated from the separated tissue slices or whole cartilage chunks via an 11 hour digestion with 390 units/mL collagenase (Type V, Sigma Aldrich) in 7.5 mL / g tissue high-glucose Dulbecco's Modified Essential Medium (hgDMEM) supplemented with 5% fetal bovine serum (FBS), essential and non-essential amino acids, buffers (HEPES, NaHCO₃) and penicillin-streptomycin (7). Superficial zone chondrocytes (SZCs) were resuspended and mixed with molten 4% or 6% type VII agarose (Sigma) in PBS at 40°C to yield a 2% and 3% agarose suspension with 30×10^6 SZCs/mL. Middle/deep zone chondrocytes (MDZCs) were resuspended and mixed with molten 4% type VII agarose (Sigma) in PBS at 40°C to yield a 2% agarose suspension with 30×10^6 MDZCs/mL. Mixed knee or CMC chondrocytes were resuspended and mixed with molten 4% type VII agarose (Sigma) in PBS at 40°C to yield a 2% agarose suspension with 30×10^6 cells/mL. Using a custom template (17), bilayered constructs ($\text{Ø}4.0 \times 2.3\text{mm}$) were created with the following arrangement: 2% agarose SZC / 2% agarose MDZC (“2S2M”) and 3% agarose SZC / 2% agarose MDZC (“3S2M”). Single layer constructs ($\text{Ø}4.0 \times 1.0\text{mm}$) of 2% agarose SZC (“2S”), 3% agarose SZC (“3S”), and 2% agarose MDZC (“2M”) were also cast along with 2% agarose mixed knee chondrocyte (“Knee”, $\text{Ø}4.0 \times 2.3\text{mm}$) and 2% agarose mixed CMC chondrocyte controls (“Wrist”, $\text{Ø}4.0 \times 2.3\text{mm}$). These controls were chosen to compare the tissue development of the zonal chondrocyte constructs with the well-established method of using mixed chondrocyte

populations in engineering articular cartilage (4–8). The gel concentration of 2% for mixed and MDZ chondrocyte constructs was chosen based on previous research that found suboptimal tissue elaboration over extended culture with agarose concentrations greater than 3% and excessive loss of synthesized matrix with gels less than 2% composition (7,17).

All constructs were cultured at 37°C and 5% CO₂ in 35 mL of chondrogenic media (high glucose DMEM, 1% ITS+, 0.1 μM dexamethasone, 110 μg/mL sodium pyruvate, 50 μg/mL L-proline, 50 μg/mL ascorbate-2-phosphate, sodium bicarbonate, and antibiotics (19)). Media was changed bi-daily. For the first 14 days in culture, 10 ng/mL of TGF-β3 (R&D Systems, Minneapolis, MN) was added with each media change (19). Day 0 mechanical testing was performed prior to TGF-β3 treatment.

Whole Construct Mechanical Testing

Mechanical testing was performed in unconfined compression between two impermeable platens in a custom material testing device as previously described (20). Constructs (n=4–5 per group, per time point) were equilibrated under a creep tare load followed by a stress relaxation test (ramp velocity: 1 μm/s) to 10% strain (based on the post-creep thickness). The compressive Young's modulus E_Y was determined from the equilibrium stress/strain response of the tissue. Following mechanical testing, bilayered and mixed chondrocyte (Knee, Wrist) samples were allowed to recover in culture media described above for 30 minutes prior to mechanical testing for inhomogeneous properties (see below). All other constructs were frozen and stored at –80°C for subsequent biochemical analysis.

Depth-dependent Mechanical Testing

Local compressive E_Y measurements of bilayered constructs were carried out on a microscopy system for mechanical testing and image correlation, as described previously (10). Due to a lower limit on sample size (thickness > 1.5mm) imposed by the device design, only bilayered and mixed chondrocyte constructs were tested for local mechanical properties. Briefly, each disk was cut in half diametrically and one half was loaded onto a custom unconfined compression device mounted on the motorized stage of an inverted microscope. The untested half was fixed and stored for histology as described below. The initial uncompressed thickness (h_0) of the specimen was measured optically and an axial tare strain of 5% of the initial sample thickness was applied at 1 μm/s. The sample was allowed to equilibrate for 20 minutes, where images of the sample cross-section were then taken. An additional compression of 5% was then applied and a second set of images were acquired after allowing the sample to equilibrate again for 20 minutes. The entire sample cross-section was stitched using Panavue Image Assembler (Panavue, Quebec, Canada). Image analyses were performed using an optimized digital image correlation technique producing accurate axial displacements (considered to be the z-axis) and axial strain fields ($\epsilon_{zz}(z)$) (10), where $E_Y(z) = \sigma_{zz} / \epsilon_{zz}(z)$ and σ_{zz} is the normal stress measured on the specimen surface. In the presentation of results, depth is normalized to the construct thickness (z/h_0). Following testing, all specimens were frozen at –80°C for biochemical analysis. Prior to storage, bilayered samples were sharply dissected into thirds (SZC layer, interface, MDZC layer) to separate the layers (2S2M → 2S2M S, 2S2M M, 3S2M → 3S2M S, 3S2M M) and avoid layer contamination prior to freezing and storage for biochemical assays; the interface was not analyzed.

Biochemical Analysis

The samples were thawed, weighed wet, and digested for 16 h at 56°C with 1 mg/mL proteinase K (EMD Biosciences, San Diego CA) in Tris buffered saline containing EDTA, iodoacetamide and pepstatin A (Sigma Aldrich) (21). These digests were used to determine sample GAG content via the DMMB assay (22)}, DNA content via the PicoGreen assay (Invitrogen, Carlsbad, CA), and collagen content via the orthohydroxyproline colorimetric assay (23).

Collagen content was calculated by assuming a 1:10 OHP-to-collagen mass ratio (24). Assays were adapted for use in 96-well, micro-titer plates. GAG and collagen content was normalized to the construct wet weight (% ww).

Histology

Histological analysis was performed on bilayered samples to study differences in matrix formation between the zonal chondrocyte-seeded layers. Samples were fixed in acid-ethanol-formalin (25) for 48 h at 4°C, dehydrated, cleared, embedded in Tissue Prep embedding media (Fisher Scientific, Pittsburgh, PA), and sectioned at 6 µm. Sections were then stained in Safranin O and Picrosirius Red to study proteoglycan and collagen distribution.

To visualize the distribution of superficial zone protein (SZP) in the bilayered constructs, sections were stained as described previously by Krishnan et al. (26). Briefly, sections were dewaxed, rehydrated, washed in PBS (3x, 2 min each), and then blocked with 10% normal goat serum (NGS, in PBS) for 10 min at room temperature, followed by incubation with primary, rabbit-derived antibody (06A10, kindly provided by Dr Carl Flannery, Wyeth Research Division, Cambridge, MA) at a concentration of 24 µg/mL in 10% NGS for 12 h at 4°C. Antigen extraction via hyaluronidase (27) was found to be unnecessary for SZP staining (preliminary study, not shown). Sections were then washed with PBS, and incubated with Alexa Fluor 488 conjugated goat anti-rabbit secondary antibody (Molecular Probes, Eugene, OR) at 10 µg/mL in 10% NGS for 1 h at room temperature. After washing with dH₂O, samples were then treated with Propidium Iodide Nucleic Acid Stain (Molecular Probes) at 10 µg/mL for 5 min to visualize nuclei, washed 3X with dH₂O, and cover-slipped with Gel/Mount (Biomedica, Foster City, CA). On each slide, one section was maintained as a non-immune control, following the procedure described above with 10% NGS substituted for primary antibody.

Statistical Analysis

Statistics were performed using the Statistica (Statsoft, Inc., Tulsa, OK) software package. At least 4–5 samples in each group were analyzed for each data point, with data reported as the mean and standard deviation. Groups were examined using multivariate analysis of variance with E_γ, GAG, or collagen as the dependent variables, and culture time, construct group, and axial position (for local modulus data only) as the independent variables. Fisher's least-significant difference (LSD) post hoc tests were carried out with statistical significance set at $\alpha=0.05$.

Results

Gross Morphology of Zonal Chondrocytes and Engineered Constructs

Immediately after zonal chondrocyte isolation, an aliquot from the cell suspensions was viewed to observe cell morphology. Chondrocytes isolated from the superficial zone slices of cartilage tissue measured 6 ± 1 µm in diameter. In comparison, chondrocytes isolated from middle/deep zone slices measured 12 ± 2 µm in diameter (Figure 1).

Gross examination of the constructs on day 42 (Figure 2) found that the tissue elaboration, as indicated by the change in construct appearance from a translucent gel to an opaque, whitish tissue similar to that of cartilage (20), found that the SZC-only constructs (2S and 3S) possessed less cartilage tissue formation compared to MDZC-containing constructs. The 2S and 3S groups had a translucent appearance that was similar to early time point constructs. In contrast, 2M constructs possessed a shiny, opaque, white appearance similar to articular cartilage and significantly larger dimensions than either SZC construct (2M: $\text{Ø}4.06 \pm 0.05 \times 1.21 \pm 0.05$ mm; 2S: $\text{Ø}3.76 \pm 0.12 \times 1.00 \pm 0.01$ mm; 3S: $\text{Ø}3.74 \pm 0.04 \times 1.03 \pm 0.04$ mm; $p < 0.05$). Control mixed knee and wrist chondrocyte constructs (not shown) were also found to be opaque and cartilage-

like in appearance. Bilayered constructs (2S2M, 3S2M) exhibited very opaque MDZC layers and somewhat less opaque SZC layers, though these were more opaque than the SZC-alone constructs (Figure 2). On day 42, the SZC layer of the bilayered constructs was thicker in the higher gel concentration (3S2M S: 1.45 ± 0.05 mm; 2S2M S: 1.10 ± 0.07 mm; $p < 0.05$).

Biochemistry and Histology of Engineered Tissues

GAG content for all groups increased on day 14 compared to initial day 0 values (Figure 3). After day 14, the 2S group showed no further increases in tissue GAG content and exhibited the lowest GAG values of all groups on day 28 (0.55 ± 0.28 % ww) and 42 (0.90 ± 0.18 % ww). The SZC layer of the bilayered constructs (2S2M S, 3S2M S) possessed significantly greater GAG content than SZC-only, single-layer constructs (2S, 3S, $p < 0.05$). On day 14, 2S2M S (1.38 ± 0.22 % ww) and 3S2M S (1.78 ± 0.27 % ww) possessed comparable GAG content to respective 2M (1.86 ± 0.25 % ww), Knee (2.00 ± 0.10 % ww), and Wrist (1.70 ± 0.17 % ww). Engineered cartilage with MDZCs (2M, 2S2M M, 3S2M M, Knee, Wrist) in general possessed the highest GAG contents. On day 14, 3S2M M possessed the highest GAG content of that time point (2.94 ± 0.11 % ww, $p < 0.05$). Day 42 values for 2S2M M (6.73 ± 0.82 % ww) and 3S2M M (6.40 ± 1.06 % ww) showed higher GAG content than the 2M constructs alone (5.29 ± 0.42 % ww, $p < 0.05$).

Similar to tissue GAG content, the collagen content of all groups increased on day 14 over initial values (Figure 4). Engineered cartilage with MDZCs (2M, 2S2M M, 3S2M M, Knee, Wrist) in general possessed the highest collagen content, with no statistical differences between these groups and a maximal value of ~ 3.7 % ww. The 3S group possessed greater collagen than the 2S group on day 28 (0.81 ± 0.11 vs. 0.26 ± 0.06 % ww, $p < 0.05$) and on day 42 (0.85 ± 0.29 vs. 0.46 ± 0.13 % ww, $p < 0.05$). In addition, bilayered SZC layers (2S2M S, 3S2M S) on day 28 and 42 possessed greater collagen content than their single-layer counterparts (2S, 3S; Figure 4, $p < 0.05$). DNA content for all groups (normalized to day 0 values, 7935 ± 128 ng/construct) increased $\sim 20\%$ on day 14 compared to day 0 and held steady for all groups except 2M, which on day 42 possessed $\sim 40\%$ greater DNA content than initial day 0 values (Figure 5, 2M: 11362 ± 421 ng/construct).

Day 42 histology of bilayered constructs (Figure 6) showed greater GAG content in the MDZC layers than the SZC layers of both 2S2M and 3S2M constructs. The SZC layer of 3S2M showed greater GAG and thickness than the respective layer in 2S2M. Some GAG loss was noted on all construct edges. The SZC layer of the 3S2M showed greater collagen content than the 2S2M, though it appeared that the MDZC of both possessed more collagen.

Immunohistochemistry for SZP (Figure 7) found the presence of the protein localized with the cells on the superficial ~ 200 μ m of the SZC layers in both 2S2M and 3S2M constructs, with stronger intensity of staining in 3S2M. Dispersed SZP with low staining intensity was found in Knee constructs with a mixed-population of chondrocytes. This staining, however, was consistent with negative-immune control Knee construct slides. No SZP protein was found in the MDZC layers of either bilayered constructs or in their negative control slides (not shown).

Mechanical Properties of Constructs

Constructs in the 2S, 3S, and 2S2M groups did not show any significant increases in E_Y from day 0 values over the 42 day culture duration (Figure 8). The 2M group exhibited significant increases in E_Y on day 14 and 42, reaching a final value of 142.9 ± 35.7 kPa. The 3S2M bilayered group exhibited increases in compressive E_Y on day 14, 28, and 42, reaching a value of 106.2 ± 34.8 kPa. Mixed chondrocyte tissues (Knee and Wrist) increased in compressive E_Y on days 14, 28, and 42 and Wrist constructs attained the highest mechanical properties,

625.4 ± 35.7 kPa, on day 42. At this time point, Knee chondrocyte constructs were at 425.1 ± 29.3 kPa.

Depth-dependent Material Properties

On day 0, mixed population constructs possessed uniform local mechanical properties and bilayered constructs showed two regions each with uniform properties with values determined by the intrinsic properties of the agarose gel (not shown). This was consistent with previously reported results (17). After 42 days in culture, mixed population chondrocytes possessed a U-shaped profile in depth-varying E_Y . This profile indicated that the top and the bottom faces of the constructs (normalized depths $z/h_0=0$ and 1) possessed the highest local E_Y (peak local E_Y : Knee ~ 425 kPa, Wrist ~ 800 kPa) and the central regions possessed the lowest values ($z/h_0 = 0.4-0.6$, Knee ~ 150 kPa, Wrist ~ 300 kPa). Wrist constructs were significantly stiffer by nearly 2-fold at all locations compared to Knee constructs (Figure 9 A, B; $p < 0.05$). Bilayered constructs at this time point showed a profile of E_Y that increased from the SZC layer to the MDZC layer (Figure 9 C), with the bottom face ($z/h_0=0.9$) of the MDZC layers in both constructs attaining the highest local E_Y (~ 350 kPa). This profile appears qualitatively similar to the measurements made on native articular cartilage (Figure 9 D) (9,28). The SZC layer ($z/h_0=0-0.5$) of 3S2M constructs possessed a significantly higher E_Y ($\sim 40-150$ kPa @ $z/h_0=0-0.5$) compared to 2S2M constructs ($\sim 15-90$ kPa, $p < 0.05$).

Discussion

The protocol utilized in this study is the first in the literature, as known to the authors, to produce a bilayered cartilage construct (2S2M and 3S2M) with zonal chondrocyte organization and depth-dependent mechanical inhomogeneity that is qualitatively similar to the native tissue (9,10), which affirms the study hypothesis. The compressive properties and GAG content of the 3S2M bilayered constructs were found to be in the physiologic range for full thickness knee tissue (29) and appear to represent the highest values reported so far for layered, engineered cartilage (13,16,30). The development of a mechanically competent tissue prior to *in vivo* implantation may be clinically relevant as a soft construct may not be able to preserve the prescribed cell stratification and prevent host cell infiltration (31).

These results represent the first reported by our laboratory for knee chondrocytes and for zonal chondrocyte populations, requiring the validation of the employed methodology. Examination of the chondrocytes post-digestion was used to quickly confirm that the zonal chondrocytes were indeed isolated using the techniques adapted from Kim et al. (12). Engineered cartilage containing CMC chondrocytes was included to allow comparisons with previous published results from our laboratory (18,32). Engineered cartilage produced from mixed populations of knee chondrocytes possessed lower compressive modulus than their CMC counterparts. This is likely due to known differences in chondrocytes isolated from different anatomic locations (33,34). Interestingly, though the mechanical properties differed, mixed knee and wrist chondrocytes synthesized similar amounts of GAG and collagen. Therefore, it is likely that the disparate compressive stiffness between the two groups is due to unmeasured differences in the structure and species of matrix constituents between the knee and wrist chondrocytes. This has larger implications that the location from which cells are harvested may directly impact the success of cell-based therapies to repair damaged articular cartilage.

The analysis of the layers in the bilayered constructs found a synergistic increase in GAG content in both the SZC and MDZC layers when compared to the chondrocyte populations cultured separately. The differences in the GAG content between the constructs would lead to differing swelling pressures within the tissue (35-37), explaining the observed differences in construct/layer size. Though it may be argued that the increase in the GAG content of the SZC layer in a bilayered construct, compared to the SZC-alone construct, may be due to GAG

diffusion from the MDZC layer, the fact that the GAG content of the MDZC layer also increased would strongly suggest that cellular communication and GAG upregulation is indeed present. This could be further verified by radiolabeled sulfate incorporation measurements in the future. Interestingly, there was no change in collagen content in the MDZC layers of the bilayered constructs, indicating that different pathways were upregulated with SZC communication. The measured collagen content of all experimental groups was lower than native cartilage values (38), a pervasive problem in cartilage tissue engineering. In general, however, the low collagen content, appears to result not from amino acid deficiencies in the culture media (39), but rather the lack of an appropriate stimulatory signal (40).

There was a regulation of MDZC proliferation when cultured in the presence of the SZCs. The GAG and proliferation results are consistent with previously reported findings by Sharma et al. with knee SZCs and DZCs seeded in a layered PEG gel and cultured in the presence of fetal bovine serum (16). However, these authors also reported synergistic increases in collagen content when SZCs and DZCs were layered together, a finding that was not observed in the current study. Interestingly, scaffold-free layered constructs (13) with knee SZCs and MZCs, cultured in fetal bovine serum, showed no synergistic increases in matrix synthesis or in DNA regulation, contrary to the results reported here and the work of Sharma et al. These differences, though utilizing chondrocytes isolated from the same general anatomic location, are likely due to differences in culture conditions (such as serum or no serum), duration, and potential interactions with the scaffold material.

The use of 3% agarose to encapsulate SZCs appeared to increase the GAG and collagen content compared to 2% agarose in both bilayered and monolayered constructs. It is known that SZCs synthesis less GAG and produce smaller aggregated proteoglycans than middle or deep zone chondrocytes (41). It is therefore likely that the decreased porosity and permeability in 3% agarose versus 2% agarose (17,42,43) lead to increased entrapment of the secreted biomolecules, including SZP as seen in the bilayered constructs (Figure 7). This would indicate that tailoring the scaffold properties to the seeded cell phenotype can optimize the retention of synthesized matrix. To directly confirm this, future studies would need to track the amounts of GAG in the media as well as that retained by the tissue, and/or direct measurements of total GAG synthesis, such as sulfate incorporation.

This study is the first, to the best of our knowledge, to report a depth-dependent inhomogeneity in the compressive Young's modulus that resembles the native tissue in a zonal chondrocyte seeded construct. This inhomogeneity likely affected the measured E_Y of the intact bilayered constructs as the softer SZC layer would greatly influence the measurements given the small applied strain (10%) during whole-construct testing of the intact specimens. In contrast to the bilayered constructs, mixed chondrocyte constructs possessed a U-shaped, local E_Y profile. This profile is consistent with previously published reports (44) and indicates greater matrix accumulation and/or organization at the edges than in the center of the disk. In a scaffold-free construct with zonal chondrocyte populations, the depth-dependent inhomogeneity formed was not similar to the native cartilage (15). This finding in the literature, combined with the present results, implies that a scaffold may be necessary to develop this aspect of the native tissue in an engineered construct. Given the limited research in this area, the functional benefits of depth-dependent inhomogeneity in engineered cartilage are not clear. In theoretical modeling of articular cartilage (29), a small (~5%) increase in the fluid load support at the articular surface was found due to depth-dependent material properties and this effectively halved the surface friction coefficient. Therefore, frictional testing (45) on the bilayered constructs is planned to explore this possibility. As the fluid load support mechanism in articular cartilage is dependent on the ratio of tensile and compressive properties, tensile measurements utilizing osmotic swelling and the microscope testing device (46) will also be included in the future to determine the depth-dependent tensile properties of the bilayered tissues.

The presence of SZP at the articulating surface of engineered cartilage may be of direct clinical benefit. Though superficial zone protein is believed to act as a boundary lubricant (47), SZP may be more important clinically for its role in preventing wear and cartilage-cartilage adhesion (48,49). Knock-out mice for the PRG4 gene, which encodes for SZP, showed surface degeneration and synoviocyte overgrowth that led to joint failure (49). These issues were ameliorated with treatment of lubricin, a homolog of SZP. Clearly, in the repair of a focal defect, the host tissue SZCs will still exist and produce SZP that may, in turn, protect the surfaces of the implanted engineered cartilage. However, for large defect repair and proposed engineered tissue arthroplasty (50), the addition of a layer of SZC to the engineered cartilage may be critical in joint repair and restoration of function. In conjunction with the proposed *in vitro* friction testing, future *in vivo* studies are planned to evaluate any beneficial impact of SZCs in engineered tissue in regards to the clinical measures of joint function and mobility in repaired knee defects (e.g., gait, congruence, filling, adhesions, etc.). Interestingly, no significant SZP expression was found in mixed Knee chondrocyte constructs. Given that only the topmost SZCs in the layered constructs expressed SZP, this finding in the mixed chondrocytes Knee constructs would imply that the expression of SZP can be modulated by the middle/deep zone chondrocytes. The mechanism may be direct cell-to-cell communication as a soluble factor would have affected all of the SZCs in the layered construct.

Zonal chondrocytes encapsulated in a bilayered agarose construct with initially prescribed mechanical inhomogeneity formed an engineered cartilage that possessed depth-dependent cellular and compressive mechanical inhomogeneity similar to that of the native tissue. The results obtained affirm the study hypothesis and the principle that targeted scaffold design in combination with cell selection can further improve the creation of a biomimetic engineered cartilage tissue. The methodology employed represents a first attempt to recapitulate the depth-dependent cellular and mechanical inhomogeneity of native articular cartilage in an engineered construct. With the bilayered construct created in this study, it will be possible to evaluate using future *in vivo* experiments the functional benefits and necessity of depth-dependent cellular and mechanical inhomogeneity with the ultimate goal of creating an engineered cartilage to treat osteoarthritis and degraded cartilage tissue.

Acknowledgments

The authors would like to thank Dr. Carl Flannery (Wyeth, Cambridge, MA) for providing the SZP antibody. This study was supported by the National Institute of Arthritis and Musculoskeletal and Skin Diseases of the National Institutes of Health (AR46568 and AR52871).

References

1. Freed LE, Guilak F, Guo XE, Gray ML, Tranquillo R, Holmes JW, Radisic M, Sefton MV, Kaplan D, Vunjak-Novakovic G. Advanced tools for tissue engineering: scaffolds, bioreactors, and signaling. *Tissue Eng* 2006;12:3285. [PubMed: 17518670]
2. Ingber DE, Mow VC, Butler D, Niklason L, Huard J, Mao J, Yannas I, Kaplan D, Vunjak-Novakovic G. Tissue engineering and developmental biology: going biomimetic. *Tissue Eng* 2006;12:3265. [PubMed: 17518669]
3. Mikos AG, Herring SW, Ochareon P, Elisseeff J, Lu HH, Kandel R, Schoen FJ, Toner M, Mooney D, Atala A, Van Dyke ME, Kaplan D, Vunjak-Novakovic G. Engineering complex tissues. *Tissue Eng* 2006;12:3307. [PubMed: 17518671]
4. Gooch KJ, Blunk T, Courter DL, Sieminski AL, Bursac PM, Vunjak-Novakovic G, Freed LE. IGF-I and mechanical environment interact to modulate engineered cartilage development. *Biochem Biophys Res Commun* 2001;286:909. [PubMed: 11527385]
5. Martin I, Suetterlin R, Baschong W, Heberer M, Vunjak-Novakovic G, Freed LE. Enhanced cartilage tissue engineering by sequential exposure of chondrocytes to FGF-2 during 2D expansion and BMP-2 during 3D cultivation. *J Cell Biochem* 2001;83:121. [PubMed: 11500960]

6. Masuda K, Sah RL, Hejna MJ, Thonar EJ. A novel two-step method for the formation of tissue-engineered cartilage by mature bovine chondrocytes: the alginate-recovered-chondrocyte (ARC) method. *J Orthop Res* 2003;21:139. [PubMed: 12507591]
7. Mauck RL, Soltz MA, Wang CC, Wong DD, Chao PH, Valhmu WB, Hung CT, Ateshian GA. Functional tissue engineering of articular cartilage through dynamic loading of chondrocyte-seeded agarose gels. *J Biomech Eng* 2000;122:252. [PubMed: 10923293]
8. Vunjak-Novakovic G, Martin I, Obradovic B, Treppo S, Grodzinsky AJ, Langer R, Freed LE. Bioreactor cultivation conditions modulate the composition and mechanical properties of tissue-engineered cartilage. *J Orthop Res* 1999;17:130. [PubMed: 10073657]
9. Schinagl RM, Gurskis D, Chen AC, Sah RL. Depth-dependent confined compression modulus of full-thickness bovine articular cartilage. *J Orthop Res* 1997;15:499. [PubMed: 9379258]
10. Wang CC, Deng JM, Ateshian GA, Hung CT. An automated approach for direct measurement of two-dimensional strain distributions within articular cartilage under unconfined compression. *J Biomech Eng* 2002;124:557. [PubMed: 12405599]
11. Aydelotte MB, Kuettner KE. Differences between sub-populations of cultured bovine articular chondrocytes. I. Morphology and cartilage matrix production. *Connect Tissue Res* 1988;18:205. [PubMed: 3219850]
12. Kim TK, Sharma B, Williams CG, Ruffner MA, Malik A, McFarland EG, Elisseeff JH. Experimental model for cartilage tissue engineering to regenerate the zonal organization of articular cartilage. *Osteoarthritis Cartilage* 2003;11:653. [PubMed: 12954236]
13. Klein TJ, Schumacher BL, Schmidt TA, Li KW, Voegtline MS, Masuda K, Thonar EJ, Sah RL. Tissue engineering of stratified articular cartilage from chondrocyte subpopulations. *Osteoarthritis Cartilage* 2003;11:595. [PubMed: 12880582]
14. Waldman SD, Grynepas MD, Pilliar RM, Kandel RA. The use of specific chondrocyte populations to modulate the properties of tissue-engineered cartilage. *J Orthop Res* 2003;21:132. [PubMed: 12507590]
15. Klein TJ, Chaudhry M, Bae WC, Sah RL. Depth-dependent biomechanical and biochemical properties of fetal, newborn, and tissue-engineered articular cartilage. *J Biomech* 2007;40:182. [PubMed: 16387310]
16. Sharma B, Williams CG, Kim TK, Sun D, Malik A, Khan M, Leong K, Elisseeff JH. Designing zonal organization into tissue-engineered cartilage. *Tissue Eng* 2007;13:405. [PubMed: 17504064]
17. Ng KW, Wang CC, Mauck RL, Kelly TA, Chahine NO, Costa KD, Ateshian GA, Hung CT. A layered agarose approach to fabricate depth-dependent inhomogeneity in chondrocyte-seeded constructs. *J Orthop Res* 2005;23:134. [PubMed: 15607885]
18. Lima EG, Bian L, Ng KW, Mauck RL, Byers BA, Tuan RS, Ateshian GA, Hung CT. The beneficial effect of delayed compressive loading on tissue-engineered cartilage constructs cultured with TGF-beta3. *Osteoarthritis Cartilage* 2007;15:1025. [PubMed: 17498976]
19. Byers BA, Mauck RL, Chiang I, Tuan RS. Temporal exposure of TGF-beta3 under serum-free conditions enhances biomechanical and biochemical maturation of tissue-engineered cartilage. *Trans Orthop Res* 2006;31:43.
20. Mauck RL, Wang CC, Oswald ES, Ateshian GA, Hung CT. The role of cell seeding density and nutrient supply for articular cartilage tissue engineering with deformational loading. *Osteoarthritis Cartilage* 2003;11:879. [PubMed: 14629964]
21. Riesle J, Hollander AP, Langer R, Freed LE, Vunjak-Novakovic G. Collagen in tissue-engineered cartilage: types, structure, and crosslinks. *J Cell Biochem* 1998;71:313. [PubMed: 9831069]
22. Farndale RW, Sayers CA, Barrett AJ. A direct spectrophotometric microassay for sulfated glycosaminoglycans in cartilage cultures. *Connect Tissue Res* 1982;9:247. [PubMed: 6215207]
23. Stegemann H, Stalder K. Determination of hydroxyproline. *Clin Chim Acta* 1967;18:267. [PubMed: 4864804]
24. Hollander AP, Heathfield TF, Webber C, Iwata Y, Bourne R, Rorabeck C, Poole AR. Increased damage to type II collagen in osteoarthritic articular cartilage detected by a new immunoassay. *J Clin Invest* 1994;93:1722. [PubMed: 7512992]
25. Lin W, Shuster S, Maibach HI, Stern R. Patterns of hyaluronan staining are modified by fixation techniques. *J Histochem Cytochem* 1997;45:1157. [PubMed: 9267476]

26. Krishnan R, Caligaris M, Mauck RL, Hung CT, Costa KD, Ateshian GA. Removal of the superficial zone of bovine articular cartilage does not increase its frictional coefficient. *Osteoarthritis Cartilage* 2004;12:947. [PubMed: 15564061]
27. Kelly TA, Wang CC, Mauck RL, Ateshian GA, Hung CT. Role of cell-associated matrix in the development of free-swelling and dynamically loaded chondrocyte-seeded agarose gels. *Biorheology* 2004;41:223. [PubMed: 15299255]
28. Wang CC, Chahine NO, Hung CT, Ateshian GA. Optical determination of anisotropic material properties of bovine articular cartilage in compression. *J Biomech* 2003;36:339. [PubMed: 12594982]
29. Krishnan R, Park S, Eckstein F, Ateshian GA. Inhomogeneous cartilage properties enhance superficial interstitial fluid support and frictional properties, but do not provide a homogeneous state of stress. *J Biomech Eng* 2003;125:569. [PubMed: 14618915]
30. Lee CS, Gleghorn JP, Won Choi N, Cabodi M, Stroock AD, Bonassar LJ. Integration of layered chondrocyte-seeded alginate hydrogel scaffolds. *Biomaterials* 2007;28:2987. [PubMed: 17382380]
31. Chawla K, Klein TJ, Schumacher BL, Jadin KD, Shah BH, Nakagawa K, Wong VW, Chen AC, Masuda K, Sah RL. Short-term retention of labeled chondrocyte subpopulations in stratified tissue-engineered cartilaginous constructs implanted in vivo in mini-pigs. *Tissue Eng* 2007;13:1525. [PubMed: 17532744]
32. Ng KW, Defrancis JG, Kugler LE, Kelly TA, Ho MM, O'Connor CJ, Ateshian GA, Hung CT. Amino acids supply in culture media is not a limiting factor in the matrix synthesis of engineered cartilage tissue. *Amino Acids*. 2007
33. Akens MK, Hurtig MB. Influence of species and anatomical location on chondrocyte expansion. *BMC musculoskeletal disorders* 2005;6:23. [PubMed: 15904515]
34. Hurtig MB, Fretz PB, Doige CE, Schnurr DL. Effects of lesion size and location on equine articular cartilage repair. *Canadian journal of veterinary research = Revue canadienne de recherche veterinaire* 1988;52:137. [PubMed: 3349393]
35. Maroudas A, Bayliss MT, Venn MF. Further studies on the composition of human femoral head cartilage. *Ann Rheum Dis* 1980;39:514. [PubMed: 7436585]
36. Chahine NO, Chen FH, Hung CT, Ateshian GA. Direct measurement of osmotic pressure of glycosaminoglycan solutions by membrane osmometry at room temperature. *Biophys J* 2005;89:1543. [PubMed: 15980166]
37. Lai WM, Hou JS, Mow VC. A triphasic theory for the swelling and deformation behaviors of articular cartilage. *J Biomech Eng* 1991;113:245. [PubMed: 1921350]
38. Mankin, HJ.; Mow, VC.; Buckwalter, JA.; Iannotti, JP.; Ratcliffe, A. Articular cartilage structure, composition, and function. In: Buckwalter, JA.; Einhorn, TA.; Simon, SR., editors. *Orthopaedic Basic Science. Biology and Biomechanics of the Musculoskeletal System*. Rosemont: American Academy of Orthopaedic Surgeons; 2000. p. 443-470.
39. Ng KW, Defrancis JG, Kugler LE, Kelly TA, Ho MM, O'Connor CJ, Ateshian GA, Hung CT. Amino acids supply in culture media is not a limiting factor in the matrix synthesis of engineered cartilage tissue. *Amino Acids* 2008;35:433. [PubMed: 17713744]
40. Ng KW, O'Connor CJ, Kugler LE, Ateshian GA, Hung CT. The response of engineered cartilage to a timed application of transforming and insulin-like growth factors. *Trans Orthop Res* 2008;33:588.
41. Aydelotte MB, Greenhill RR, Kuettner KE. Differences between subpopulations of cultured bovine articular chondrocytes. II. Proteoglycan metabolism. *Connect Tissue Res* 1988;18:223. [PubMed: 3219851]
42. Andarawis, NA.; Seyhan, SL.; Mauck, RL.; Soltz, MA.; Ateshian, GA.; Hung, CT. A novel device for direct permeation measurements of hydrogels and soft hydrated tissues. In: Lieber, BB., editor. *Advances in Bioengineering, BED 51*. New York: ASME; 2001. p. 299-300.
43. Gu WY, Yao H, Huang CY, Cheung HS. New insight into deformation-dependent hydraulic permeability of gels and cartilage, and dynamic behavior of agarose gels in confined compression. *J Biomech* 2003;36:593. [PubMed: 12600349]
44. Kelly TA, Ng KW, Wang CC, Ateshian GA, Hung CT. Spatial and temporal development of chondrocyte-seeded agarose constructs in free-swelling and dynamically loaded cultures. *J Biomech* 2006;39:1489. [PubMed: 15990101]

45. Krishnan R, Kopacz M, Ateshian GA. Experimental verification of the role of interstitial fluid pressurization in cartilage lubrication. *J Orthop Res* 2004;22:565. [PubMed: 15099636]
46. Chahine NO, Wang CC, Hung CT, Ateshian GA. Anisotropic strain-dependent material properties of bovine articular cartilage in the transitional range from tension to compression. *J Biomech* 2004;37:1251. [PubMed: 15212931]
47. Jay GD, Haberstroh K, Cha CJ. Comparison of the boundary-lubricating ability of bovine synovial fluid, lubricin, and Healon. *J Biomed Mater Res* 1998;40:414. [PubMed: 9570073]
48. Schaefer DB, Wendt D, Moretti M, Jakob M, Jay GD, Heberer M, Martin I. Lubricin reduces cartilage--cartilage integration. *Biorheology* 2004;41:503. [PubMed: 15299281]
49. Rhee DK, Marcelino J, Baker M, Gong Y, Smits P, Lefebvre V, Jay GD, Stewart M, Wang H, Warman ML, Carpten JD. The secreted glycoprotein lubricin protects cartilage surfaces and inhibits synovial cell overgrowth. *J Clin Invest* 2005;115:622. [PubMed: 15719068]
50. Hung CT, Lima EG, Mauck RL, Takai E, LeRoux MA, Lu HH, Stark RG, Guo XE, Ateshian GA. Anatomically shaped osteochondral constructs for articular cartilage repair. *J Biomech* 2003;36:1853. [PubMed: 14614939]

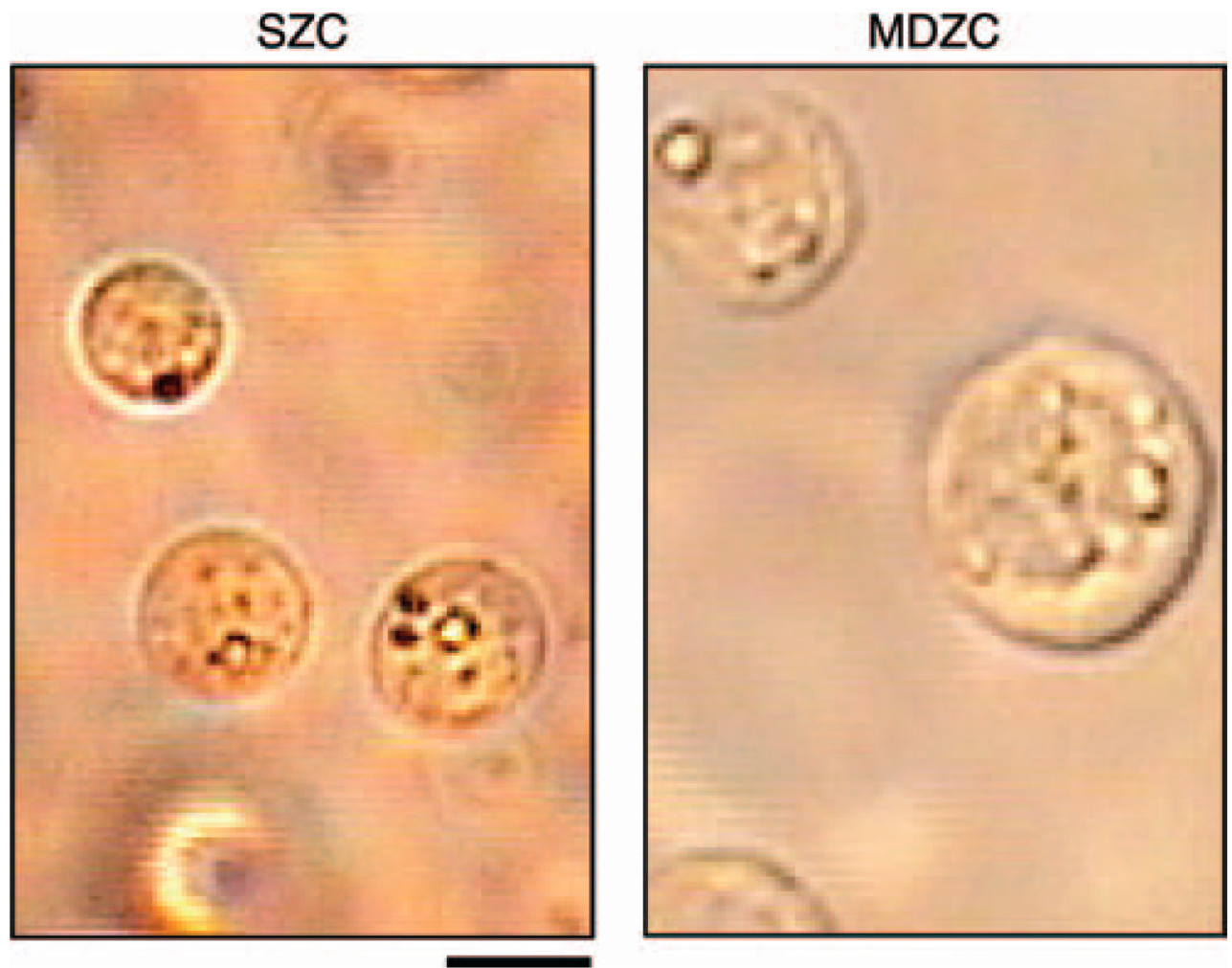


Figure 1. Gross morphology of isolated zonal chondrocyte populations. Superficial zone chondrocytes (SZC, left) immediately after isolation were smaller than middle/deep zone chondrocytes (MDZC, right), consistent with literature. Scale bar = 5 μ m.

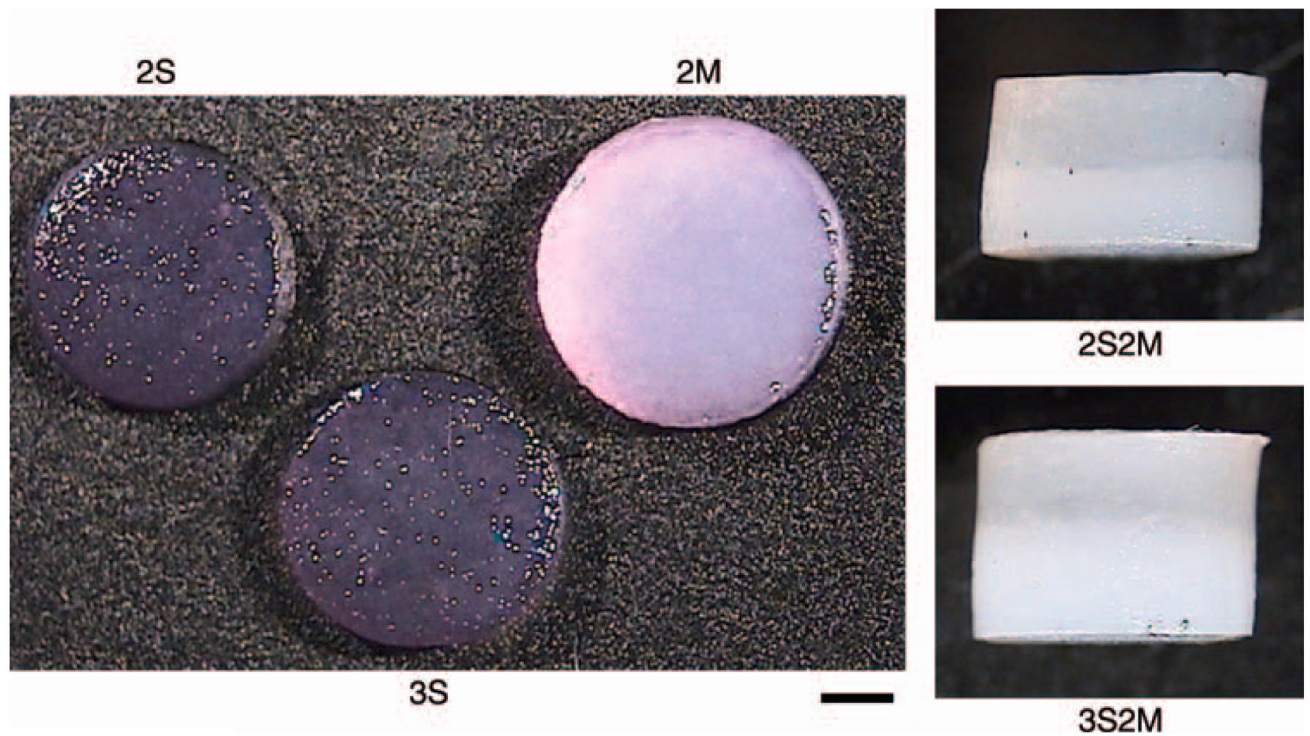


Figure 2. Gross morphology of day 42 engineered cartilage. Constructs seeded with middle/deep zone chondrocytes (2M, 2S2M, 3S2M) possessed a more opaque, whitish appearance similar to native cartilage. Scale bar = 1 mm.

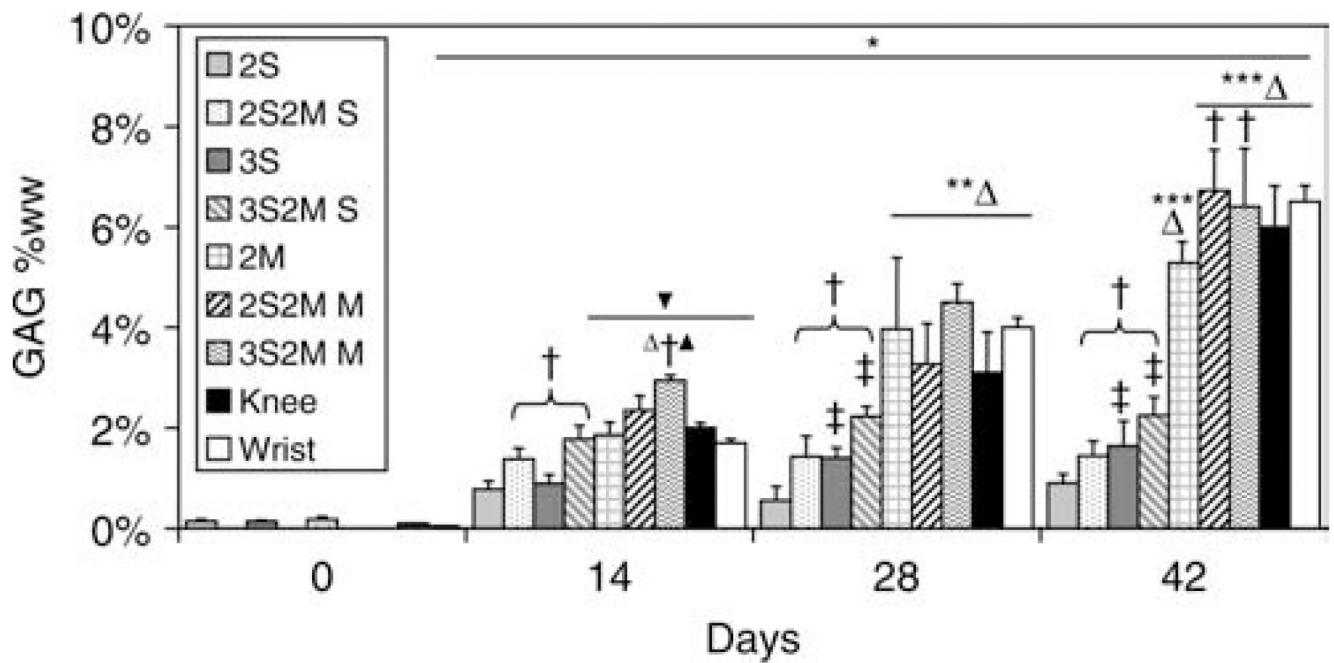


Figure 3.

GAG content of engineered cartilage constructs. For SZCs, increased agarose concentration (3S vs. 2S) and culture with MDZCs (3S2M S, 2S2M S) lead to increased GAG content. MDZCs cultured with SZCs (Knee, Wrist, 3S2M M, 2S2M M) also showed increased GAG content compared to MDZCs alone (2M). * $p < 0.05$ vs. d0; ** $p < 0.05$ vs. d14; *** $p < 0.05$ vs. d28; † $p < 0.05$ vs. respective single layer group of same time point; ‡ $p < 0.05$ vs. respective 2% gel concentration group of same time point; Δ $p < 0.05$ vs. all superficial zone chondrocyte groups of same time point; ▲ $p < 0.05$ vs. Knee and Wrist of same time point; ▼ $p < 0.05$ vs. 2S and 3S of same time point.

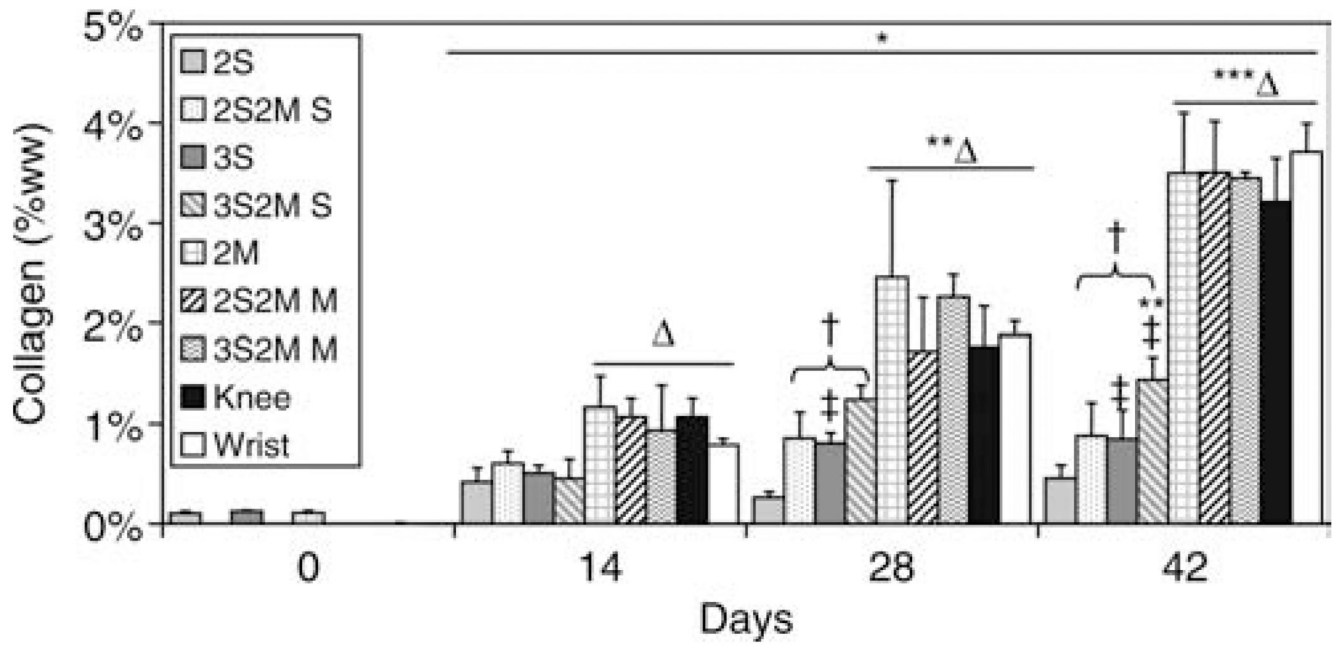


Figure 4. Collagen content of engineered cartilage constructs. For SZCs, similar effects for concentration and contact with MDZCs were noted as with GAG content. No differences were noted for MDZCs cells. * $p < 0.05$ vs. d0; ** $p < 0.05$ vs. d14; *** $p < 0.05$ vs. d28; † $p < 0.05$ vs. respective single layer group of same time point; ‡ $p < 0.05$ vs. respective 2% gel concentration group of same time point; $\Delta p < 0.05$ vs. all superficial zone chondrocyte groups of same time point.

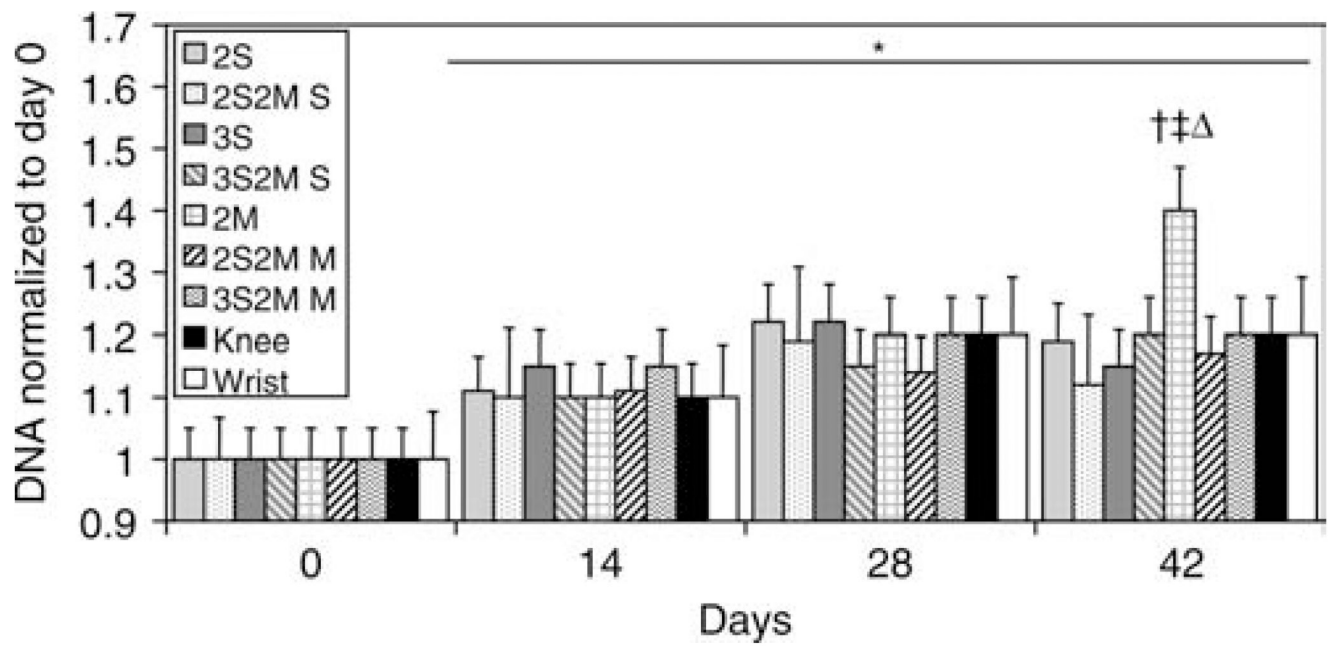


Figure 5.

The DNA content of all groups increased significantly after day 14. However, 2M constructs exhibited a further significant increase in DNA content on day 42. * $p < 0.05$ vs. d0; † $p < 0.05$ vs. d14; ‡ $p < 0.05$ vs. day 28; Δ $p < 0.05$ vs. all other groups at any time point.

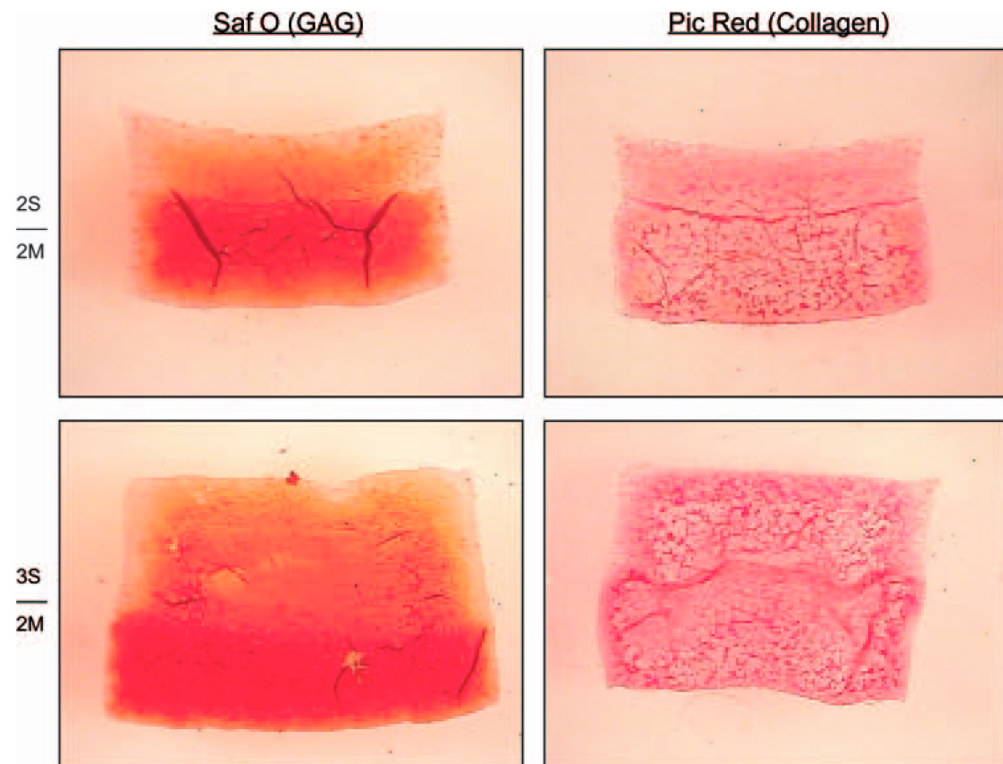


Figure 6. Histology of day 42 bilayered constructs. Safranin O (left) and Picrosirius Red (right) staining of bilayered constructs showed increased GAG and collagen in the SZC layer of 3S2M constructs as compared to 2S2M constructs. Increased GAG loss at the periphery was noted for 2S2M constructs.

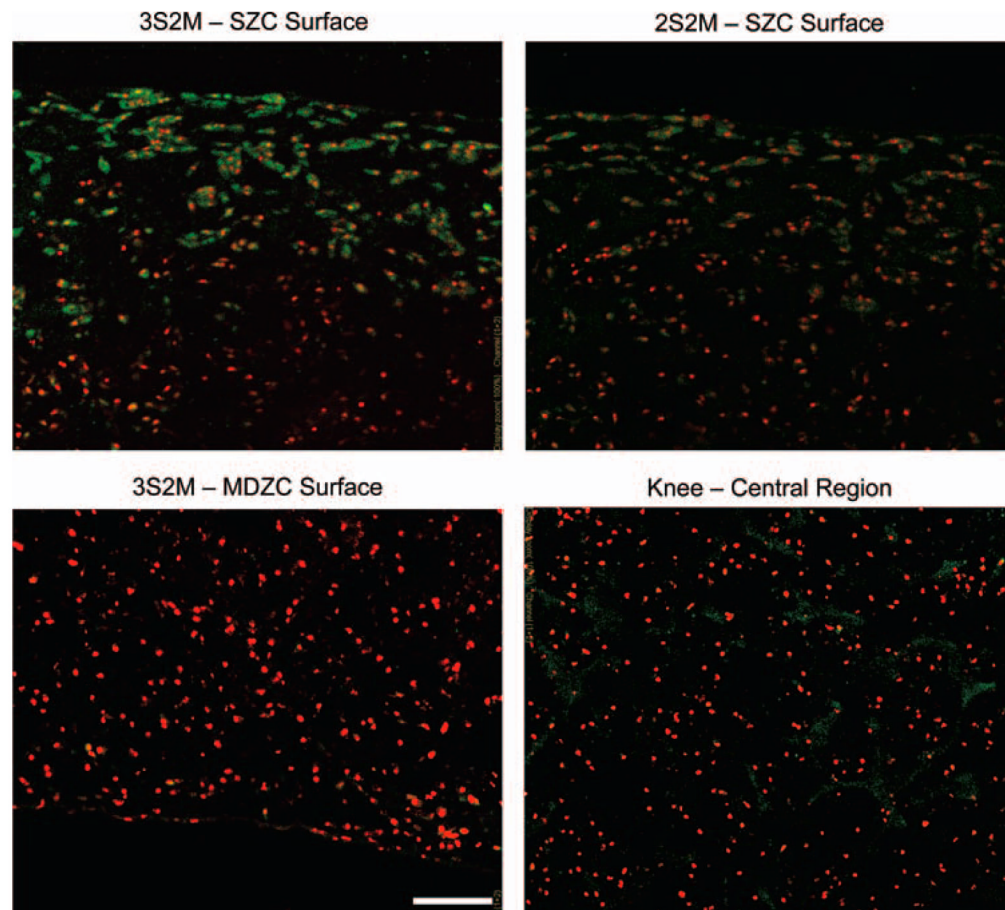


Figure 7.

SZP immunohistochemistry of bilayered and Knee constructs. SZP immunohistochemistry found the presence of the protein on the surfaces of the SZC layer of bilayered constructs. Stronger staining was found in the 3S2M construct compared to the 2S2M group. No staining for SZP was found for the MDZC layer in either bilayered group (only 3S2M shown). Dispersed SZP was found in Knee constructs with a mixed-population of chondrocytes. Scale bar = 100 μm . Cell nuclei are counterstained.

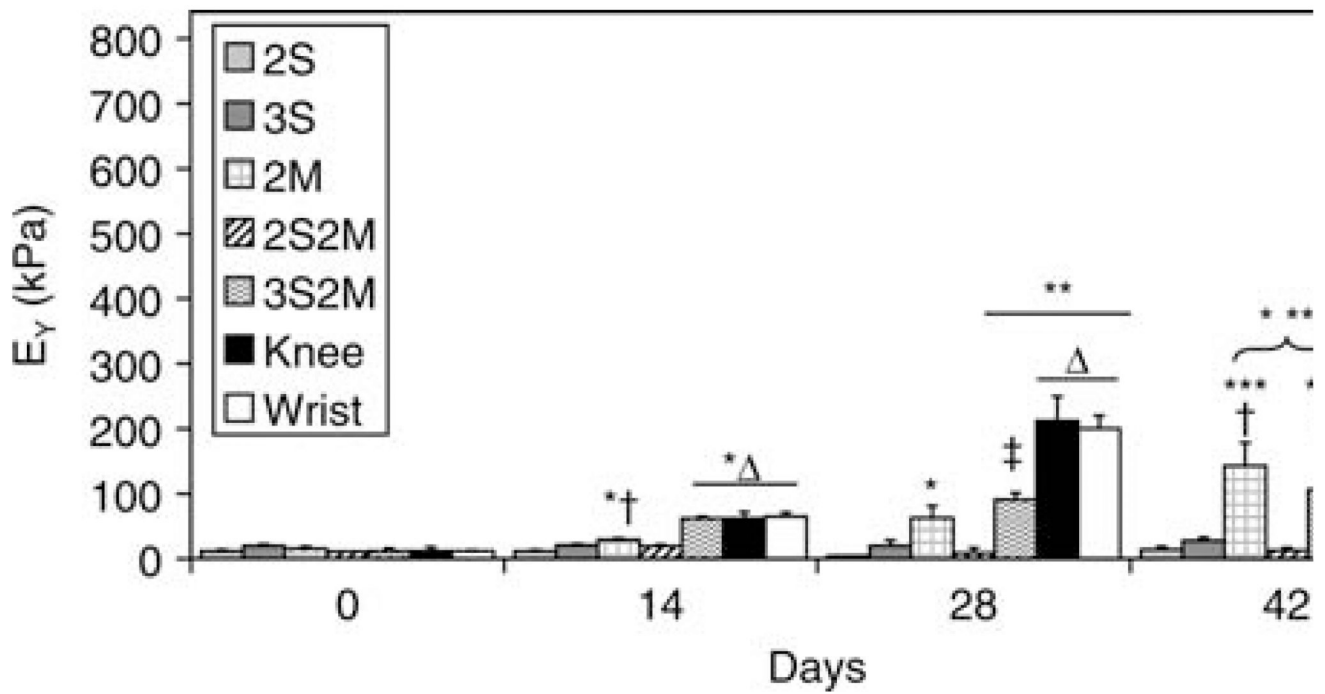


Figure 8.

Compressive Young's modulus of engineered cartilage constructs. Wrist constructs were the stiffest of all groups followed by Knee, 2M, and 3S2M tissues. The 2S, 3S, and 2S2M groups possessed the lowest compressive properties. * $p < 0.05$ vs. d0; ** $p < 0.05$ vs. d14; *** $p < 0.05$ vs. d28; † $p < 0.05$ vs. all single layer groups of same time point; ‡ $p < 0.05$ vs. all double layer groups of same time point; $\Delta p < 0.05$ vs. all other knee groups of same time point; $\blacktriangledown p < 0.05$ vs. all other groups of same time point.

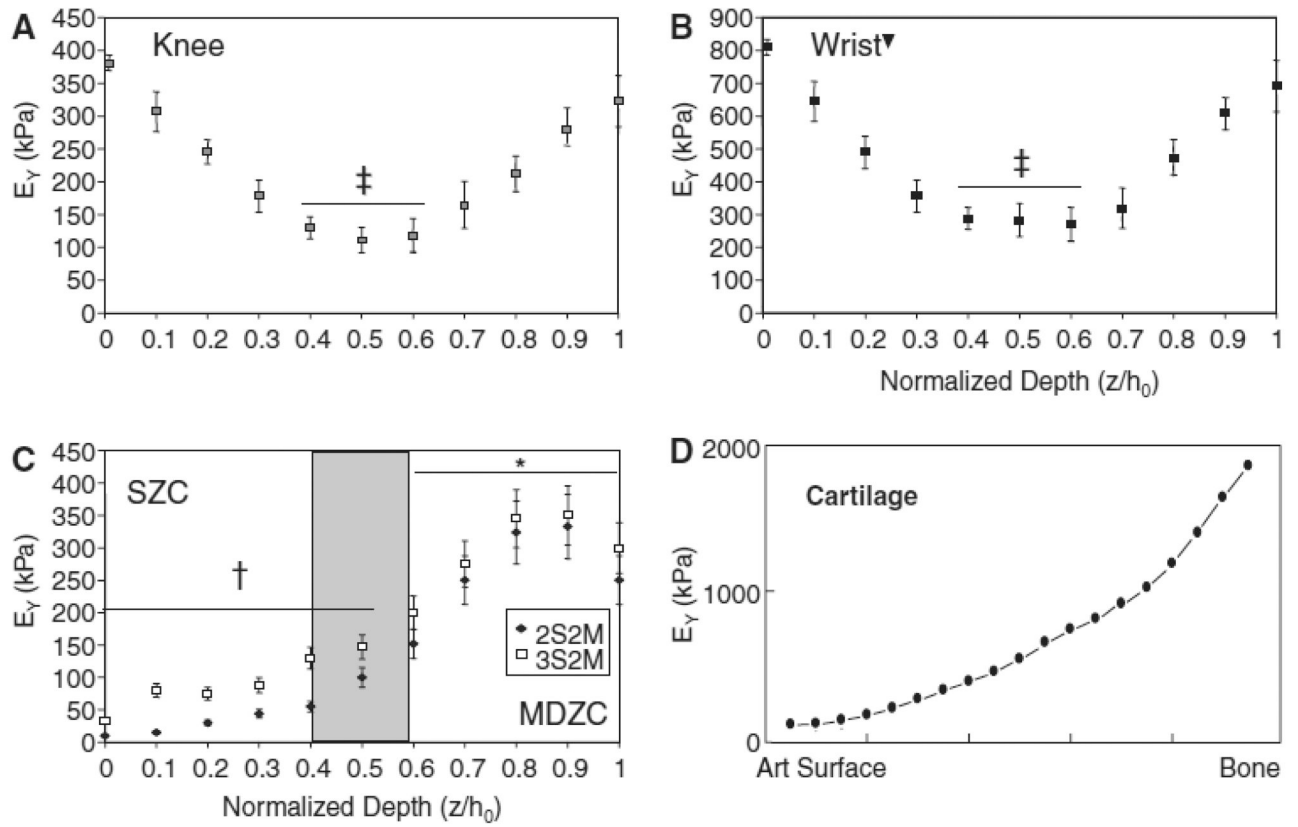


Figure 9. Local Young’s modulus for Knee (A), Wrist (B), and bilayered constructs (C). Knee and Wrist constructs possessed similar U-shaped profiles, with Wrist constructs being significantly stiffer at all locations compared to Knee. Bilayered constructs appeared to have a depth-dependent compressive E_Y that is qualitatively similar to native articular cartilage (D). * $p < 0.05$ vs. SZC layer ($z/h_0 = 0 - 0.5$); † $p < 0.05$ for 3S2M vs. 2S2M; ‡ $p < 0.05$ vs. edges ($z/h_0 = 0 - 0.1, 0.9 - 1$); ▼ $p < 0.05$ vs. all respective depths in Knee group.